Catalysis Letters, Vol. 117, Nos. 1–2, August 2007 (© 2007)
DOI: 10.1007/s10562-007-9113-x

Combined reforming of methane over supported Ni catalysts

Hyun-Seog Roh,[a] Kee Young Koo,[b] Jin Hyeok Jeong,[c] Yu Taek Seo,[a] Dong Joo Seo,[a] Yong-Seog Seo,[a] Wang Lai Yoon,[a,*] and Seung Bin Park[b]

[a]*New Energy Research Department, Korea Institute of Energy Research, 71-2, Jang-dong, Yuseong, Daejeon 305-343, Korea*
[b]*Korea Advanced Institute of Science and Technology, 373-1, Guseong-dong, Yuseong, Daejeon 305-701, Korea*
[c]*Kyungpook National University, 1370 Sankyuk-dong, Buk-gu, Daegu 702-701, Korea*

Received 30 March 2007; accepted 30 March 2007

Various supported Ni catalysts have been applied for combined steam and carbon dioxide reforming of methane to produce synthesis gas ($H_2/CO = 2$). Highly active and stable nano-sized $Ni/Mgo–Al_2O_3$ catalyst has been successfully developed for the target reaction. The high activity and stability is due to beneficial effects of MgO such as enhanced steam adsorption, basic property, nano-sized NiO crystallite size and strong interaction between Ni and support.

KEY WORDS: H_2; combined reforming; methane; Ni; catalyst.

1. Introduction

Recently, researchers are interested in hydrogen as a clean energy carrier emitting only water without co-production of greenhouse gases. Commercially, steam reforming of methane (SRM) is the primary method to produce hydrogen [1,2]. In SRM, H_2/CO ratio is higher than 3, which is not suitable for the Fischer–Tropsch and methanol syntheses. As an alternative, catalytic partial oxidation of methane (POM) to H_2 and CO has advantages such as mild exothermicity, suitable H_2/CO ratio for the Fischer–Tropsch and methanol syntheses, and very short residence time [3–7]. However, POM has disadvantages such as explosion danger and difficulty in controlling the operation. Due to these demerits, POM has not been commercialized even though it is estimated to be more economical than SRM [8].

Combined steam and carbon dioxide reforming of methane (CSCRM) offers great advantage to adjust H_2/CO ratio in the product synthesis gas to meet the requirements of downstream chemical synthesis such as Fischer–Tropsch and methanol synthesis [9]. By co-feeding steam and carbon dioxide, the H_2/CO ratio can be controlled by changing the $H_2O/CO_2/CH_4$ ratio in the reaction feed.

Commercially, supported Ni catalysts have been used in SRM because Ni is economical compared with noble metal based catalysts [1]. However, supported Ni catalysts easily deactivate due to carbon formation in carbon dioxide reforming of methane (CRM) as well as in CSCRM. Recently, Xu and co-workers reported that the Ni catalyst supported by small nanoparticles of ZrO_2 or MgO could be highly active and stable for CRM [9,10]. In addition, Roh *et al*. reported that nano-sized $Ni–Ce–ZrO_2$ catalyst could be active and stable in CRM [11,12]. Thus, it is inferred that the size of NiO and support plays a significant role in CSCRM.

In this study, various supported Ni catalysts have been prepared and applied for CSCRM to achieve a H_2/CO ratio of 2, which is suitable for the Fischer–Tropsch and methanol synthesis. We report here that nano-sized $Ni/Mgo–Al_2O_3$ catalyst exhibits the highest activity and stability among supported Ni catalysts in CSCRM due to enhanced steam adsorption, basic property, nano-sized NiO crystallite size and strong interaction between Ni and support.

2. Experimental

Supports employed in this study were $Mgo–Al_2O_3$ (MgO = 30 wt%, SASOL), MgO (99%, Kanto Chem.), ZrO_2 (99%, Fluka), CeO_2 (99%, Aldrich). $Mgo–Al_2O_3$ support was prepared by pre-calcination of hydrotalcite material at 800 °C for 6 h. The others were also pre-calcined at 800 °C for 6 h. Supported Ni catalysts (Ni = 12 wt%) were prepared by the incipient wetness method with $Ni(NO_3)_2{\cdot}6H_2O$. The prepared catalysts were calcined at 800 °C for 6 h in air. Commercial Niα-alumina catalyst was employed as a reference in CSCRM.

The BET surface area was measured by nitrogen adsorption at −196 °C using Micromeritics (ASAP 2000). The XRD patterns were recorded using a Rigaku D/MAX-IIIC diffractometer (Ni filtered Cu-Kα radiation, 40 kV, 50 mA). The crystallite size of NiO and

*To whom correspondence should be addressed.
E-mail: wlyoon@kier.re.kr

support in prepared catalysts was estimated using the Scherrer equation [13]. H_2-chemisorption was conducted in ASAP 2010 (Micromeritics). The calcined catalyst sample (about 0.2 g) was reduced at 800 °C for 1 h in H_2 flow and analyzed at 50 °C. Each point was measured after 5 min stabilization. From the chemisorbed amount, the Ni surface area was calculated by assuming the adsorption stoichiometry of one hydrogen atom per nickel surface atom ($H/Ni_s = 1$). Temperature programmed reduction (TPR) experiments were carried out in a conventional apparatus. Typically, 0.1 g of precalcined sample was loaded into quartz reactor. The TPR was performed using 10% H_2 in Ar with a heating rate of 20 °C/min, from 200 to 1000 °C. The sensitivity of the detector was calibrated by reducing known weight of NiO. H_2 consumption was obtained from the integrated peak area of the reduction profiles relative to the calibration curve.

Activity tests were carried out at 800 °C under atmospheric pressure in a fixed-bed micro-tubular quartz reactor with an inner diameter of 4 mm. The catalyst charge was 10 mg, and $MgAl_2O_4$ was used as a catalyst diluent. A thermocouple was inserted into the catalyst bed to measure the reaction temperature. Prior to each catalytic measurement, the catalyst was reduced in 10% H_2/N_2 at 700 °C for 1 h. The reactant gas stream consisted of H_2O, CO_2, and CH_4. The feed ($H_2O + CO_2$)/CH_4 ratio was fixed at 1.2. A space velocity of 265,000 cm^3 gas fed/g_{cat}-h was used to screen the catalysts in this study. Water was fed using a syringe pump and was vaporized at 150 °C upstream of the reactor. The reformate was chilled, passed through a trap to condensate residual water, and then flowed to the online gas chromatograph (HP 6890N).

3. Results and discussion

3.1. Catalyst characterization

Table 1 summarizes the characteristics of the supported Ni catalysts used in this study. The BET surface area of Ni/Mgo–Al_2O_3 is the highest among the prepared catalysts. MgO plays a role as a dopant in maintaining high surface area even after calcination at high temperature. Therefore, even though the catalyst was calcined at 800 °C for 6 h, the high surface area was maintained. On the contrary, the commercial catalyst, Niα-alumina, shows the lowest BET surface area.

Table 1
Characteristics of supported Ni catalysts

Catalyst	BET S.A. (m^2/g)	NiO crystallite size (nm)	Support size (nm)
Ni/Mgo–Al_2O_3	108	N.A.[a]	4
Ni/MgO	6	N.A.[b]	60
Ni/ZrO_2	17	21	24
Ni/CeO_2	9	55	36
Niα–Al_2O_3	4	25	77

[a] Not available due to very broad and weak XRD peaks.
[b] Not available due to overlapping with MgO peaks.

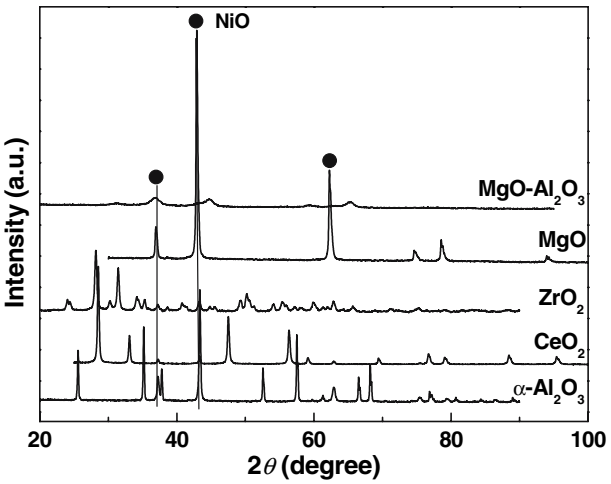

Figure 1. XRD patterns of supported Ni catalysts.

XRD patterns of supported Ni catalysts are shown in figure 1. The commercial Niα-alumina catalyst shows all characteristic reflections corresponding to NiO and α-alumina phases. For the Ni/CeO_2 catalyst, the peaks are corresponding to cubic structure of CeO_2 and NiO [11]. On the other hand, the Ni/ZrO_2catalyst shows characteristic peaks, which can be assigned to reported monoclinic structure of ZrO_2 and NiO [2]. The Ni/MgO catalyst shows the cubic structure of both NiO and MgO. Because NiO peaks overlap with MgO peaks, it is not possible to calculate the NiO size using Scherrer equation. However, the crystallite size of MgO has been calculated using the XRD pattern of MgO support. In the case of Ni/Mgo–Al_2O_3 catalyst, XRD pattern is consistent with $MgAl_2O_4$ spinel phase. The NiO crystallites are very small as the peaks due to NiO are quite broad. Therefore, NiO crystallite size could not be estimated in this catalyst composition. It means that the crystallite size of NiO is less than 3 nm, which is the detection limit of XRD. The XRD results thus confirmed fine dispersion of NiO crystallites in the spinel $MgAl_2O_4$ support.

It is noteworthy that high surface area and good dispersion of NiO crystallites in the Ni/Mgo–Al_2O_3 catalyst is obtained even after calcination at 800 °C for 6 h. As a consequence, the Ni/Mgo–Al_2O_3 catalyst shows the highest Ni surface area after reduction process (table 2). The Ni surface area estimated from H_2 chemisorption decreases in the order: Ni/MgO–Al_2O_3 > Ni/α–Al_2O_3 > Ni/ZrO_2 > Ni/CeO_2 > Ni/MgO. Both BET surface area and Ni surface area indicate that Ni is well dispersed onto Mgo–Al_2O_3 resulting in the smallest Ni crystallite size of the catalyst. By the way, the reduction degree of Ni/Mgo–Al_2O_3 is the smallest, indicating strong metal to support interaction. In the case of Ni/MgO, the reduction degree is 77%, which is

Table 2
H_2 chemisorption results

Catalyst	Ni reduction degree (%)	Dispersion (%)	Ni surface area (m^2/g)	Ni crystallite size (nm)
Ni/Mgo–Al_2O_3	56	12.0	5.6	8
Ni/MgO	77	0.3	0.2	311
Ni/ZrO_2	99	0.5	0.4	200
Ni/CeO_2	94	0.4	0.3	245
Niα–Al_2O_3	95	0.8	0.6	128

All the catalysts were reduced at 800 °C for 1 h.

second smallest value among the catalysts. On the contrary, the others show more than 94% reduction degree, indicating almost all NiO species are reducible after reduction at 800 °C.

TPR patterns of supported Ni catalysts are depicted in figure 2. It is known that the lower temperature peaks are assigned to the reduction of the relatively free NiO species, while the higher temperature peaks are attributed to the reduction of complex NiO species, which have strong interaction with support. The TPR curve of Ni/α–Al_2O_3 is similar to that of pure NiO [2], indicating that free NiO species are present on the α–Al_2O_3 support. Ni/CeO_2 shows sharp reduction peak at about 400 °C followed by a small tail. It is probable that NiO can be reduced easily in the presence of CeO_2, which agrees with the literature [14, 15]. There is another peak at 830 °C due to partial reduction of CeO_2, which is consistent with the TPR curve of only CeO_2 support [6]. For Ni/ZrO_2, reduction peaks with maxima at about 420 and 490 °C are observed. The former can be assigned to relatively free NiO species and the latter to complex NiO species. Ni/MgO shows the reduction peak at around 600 °C on account of strong Ni to support interaction. In the case of Ni/Mgo–Al_2O_3, the maximum peak shifts toward the high temperature (830 °C). This suggests that the interaction between Ni and Mgo–Al_2O_3 is the strongest among the catalysts.

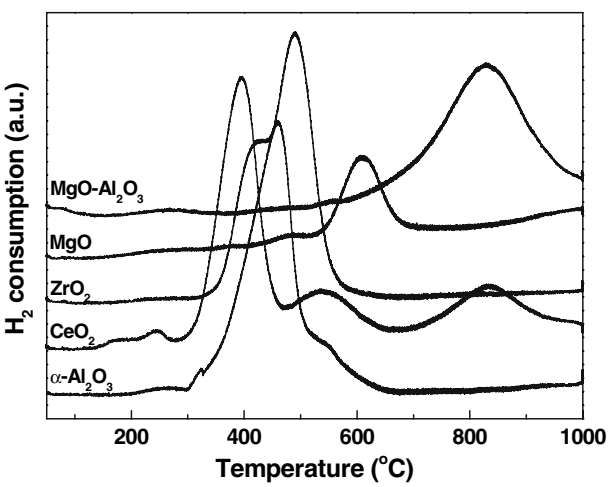

Figure 2. TPR patterns of supported Ni catalysts.

Table 3
H_2/CO ratio depending on feed $H_2O/CO_2/CH_4$ ratio

$H_2O/CO_2/CH_4$ ratio	H_2/CO ratio	
	Theoretical	Experimental
0.0/1.2/1.0	0.9	0.9
0.6/0.6/1.0	1.6	1.5
0.8/0.4/1.0	2.0	1.9
0.9/0.3/1.0	2.3	2.2
1.2/0.0/1.0	3.3	3.3

3.2. Reaction results

In order to adjust H_2/CO ratio in the product synthesis gas to be suitable for Fischer–Tropsch and methanol syntheses in CSCRM, the $H_2O/CO_2/CH_4$ ratio in the reaction feed was systematically changed. The reaction results are summarized in table 3. As can be seen in table 3, the H_2/CO ratio can be easily adjusted from 0.9 to 3.3 by controlling the feed H_2O/CO_2 ratio. In addition, experimental values are close to theoretical values. Thus, it is confirmed that the product H_2/CO ratio is adjusted by combination of SRM and CRM.

Supported Ni catalysts have been tested at 800 °C with $H_2O/CO_2/CH_4$ ratio of 0.8/0.4/1.0 and space velocity of 265,000 $cm^3/h\ g_{cat}$. The reaction results for CH_4 conversion with time on stream are presented in figure 3. It is clear that Ni/Mgo–Al_2O_3 catalyst exhibited the highest CH_4 conversion and around 90% conversion was maintained for around 20 h. In the case of commercial Niα-alumina catalyst, the catalyst rapidly deactivated with time on stream due to carbon formation. After the reaction, serious coke formation could be seen along the reactor. This is due to the fact that the commercial catalyst has been optimized for SRM, which uses excess steam to prevent coke formation [1]. It indicates that the commercial catalyst is not suitable for

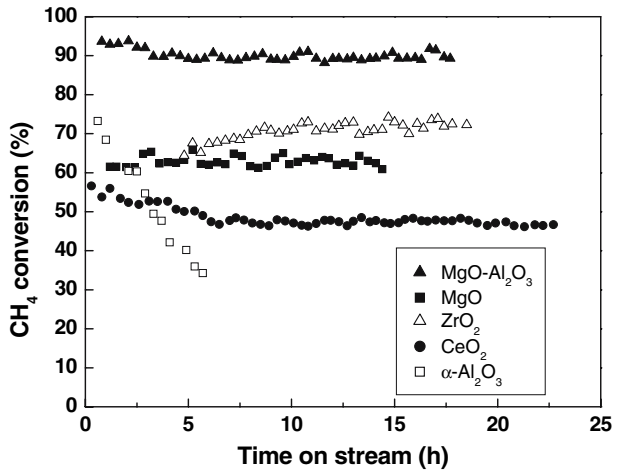

Figure 3. CH_4 conversion with time on stream over supported Ni catalysts (T = 800 °C, $H_2O/CO_2/CH_4$ ratio of 0.8/0.4/1.0).

CSCRM. Ni/MgO showed about 60% CH_4 conversion and it was maintained. So far, Ni/MgO showed fairly good activity and stability in POM [3]. By the way, Ni/ZrO_2 showed about 70% CH_4 conversion. It also showed good stability during the reaction. Ni/CeO_2 showed initially 57% CH_4 conversion, and it gradually decreased to 50% and it was maintained. Among the supported Ni catalysts used in this study, Ni/Mgo–Al_2O_3 with the smallest NiO crystallite size and Ni crystallite size exhibited the highest CH_4 conversion as well as stability with time on stream.

Figure 4 shows SEM images of used catalysts. All the catalysts showed coke formation after the reaction at 800 °C. However, the shape and degree of coke formation depended on each catalyst. Ni/MgO formed a lot of filamentous coke during the reaction. Ni/α–Al_2O_3 showed rod-like coke. Compared with coke formation over Ni/MgO and Ni/α–Al_2O_3, less amount of coke was foundin other catalysts. The Ni/Mgo–Al_2O_3 catalyst also showed filamentous coke but the degree of coke formation was not severe. In the case of Ni/ZrO_2, worm-like coke was found. For Ni/CeO_2, the same shape of coke was monitored.

Table 4
Comparison of reaction results over Ni/Mgo–Al_2O_3 and Ni/$MgAl_2O_4$

Catalyst	CH_4 conversion		CO_2 conversion	
	700 °C	650 °C	700 °C	650 °C
Ni/Mgo–Al_2O_3	83%	68%	71%	51%
Ni/$MgAl_2O_4$	62%	48%	50%	38%

In the next step, the Ni/Mgo–Al_2O_3 catalyst developed in this study was compared with the commercial Ni/$MgAl_2O_4$ catalyst at different temperatures. The results are summarized in table 4. The commercial Ni/$MgAl_2O_4$ catalyst was used as a reference catalyst. It shows 2.2% dispersion and calculated Ni crystallite is 43 nm. At 700 °C, Ni/Mgo–Al_2O_3 exhibited 83% CH_4 conversion and 71% CO_2 conversion. This is due to the

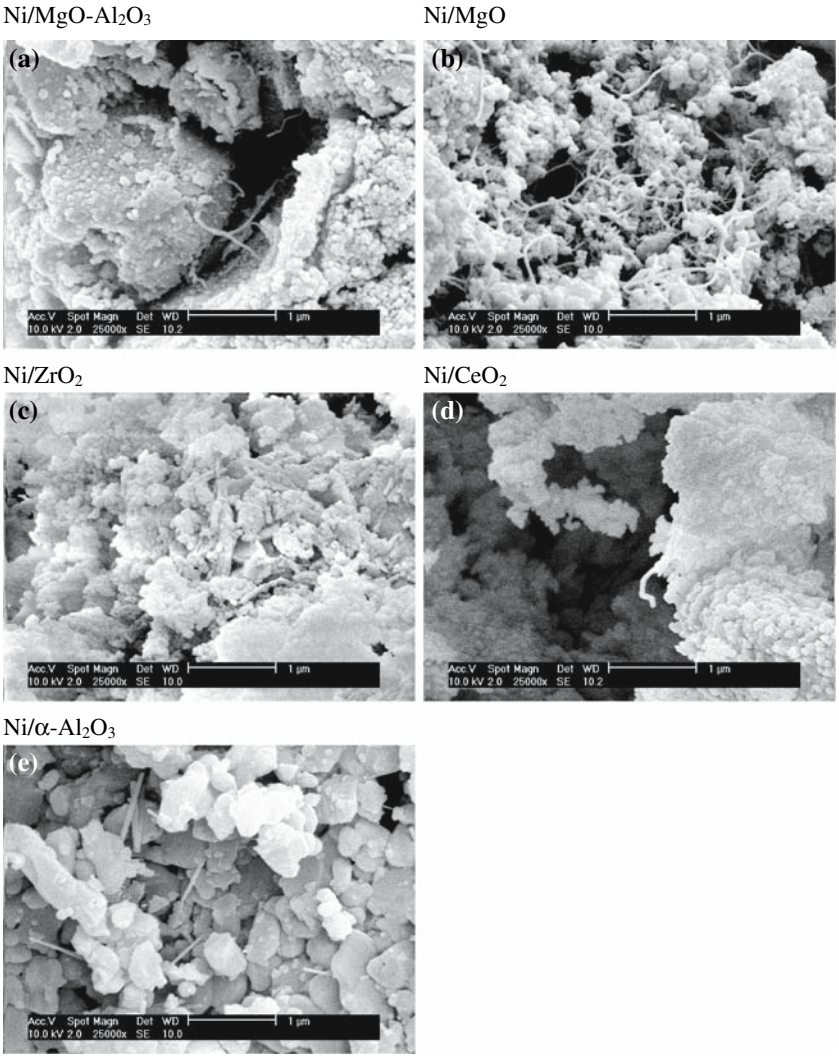

Figure 4. SEM images of used catalysts: (a) Ni/Mgo–Al_2O_3, (b) Ni/MgO, (c) Ni/ZrO_2, (d) Ni/CeO_2 and (e) Niα–Al_2O_3.

fact that steam is more reactive than CO_2 as an oxidant in the reaction condition. On the contrary, CH_4 and CO_2 conversions of $Ni/MgAl_2O_4$ were about 20% lower than those of $Ni/Mgo–Al_2O_3$. Similar trends were measured at 650 °C. Thus, it has been confirmed that $Ni/Mgo–Al_2O_3$ is different from conventional $Ni/MgAl_2O_4$, which has been used commercially in SRM.

To see coke resistance over $Ni/Mgo–Al_2O_3$ and $Ni/MgAl_2O_4$, used samples were characterized using SEM images after the reaction at 650 °C (figure 5). It is obvious that coke formation over the commercial $Ni/MgAl_2O_4$ catalyst is more severe than that over $Ni/Mgo–Al_2O_3$. It means that $Ni/Mgo–Al_2O_3$ has high coke resistance compared with $Ni/MgAl_2O_4$. This is possibly due to the high dispersion of Ni over $Mgo–Al_2O_3$. It is known that nano-sized Ni has high coke resistance in reforming reactions [12].

The fact that Ni supported on $Mgo–Al_2O_3$ showed the highest activity and stability can be explained as follows. MgO has beneficial effects as a promoter in CSCRM. First, MgO can enhance steam adsorption in reforming reactions [1]. As a result, $Ni/Mgo–Al_2O_3$ was relatively stable in CSCRM, while commercial Niα-alumina catalyst deactivated with time on stream. Second, MgO has basic property to prevent coke formation. It is known that coke formation is favorable on acid sites [1]. Third, NiO is finely dispersed on $Mgo–Al_2O_3$ resulting from high surface area of $Mgo–Al_2O_3$. This is due to the role of MgO as a dopant resulting in high thermal stability of $Mgo–Al_2O_3$. This is in good agreement with the literature [16, 17]. It is reported that hydrotalcite materials form a homogeneous mixture with very small crystal size, stable to thermal treatment, and upon reduction form small and thermally stable metal crystallites. As a consequence, the smallest NiO crystallite size is achieved, resulting in the smallest Ni crystallite size after reduction. Fourth, there is strong metal to support interaction (SMSI). This is confirmed from TPR curve of $Ni/Mgo–Al_2O_3$. As a consequence, sintering of active sites may be avoided resulting in stability during the reaction. It is also reported that the free NiO species, which has no interaction with support, is responsible for coke formation in CRM [18, 19].

$Ni/MgO-Al_2O_3$

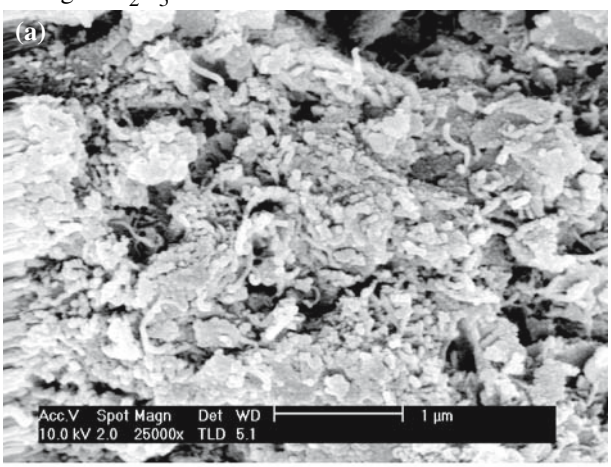

Commercial $Ni/MgAl_2O_4$ catalyst

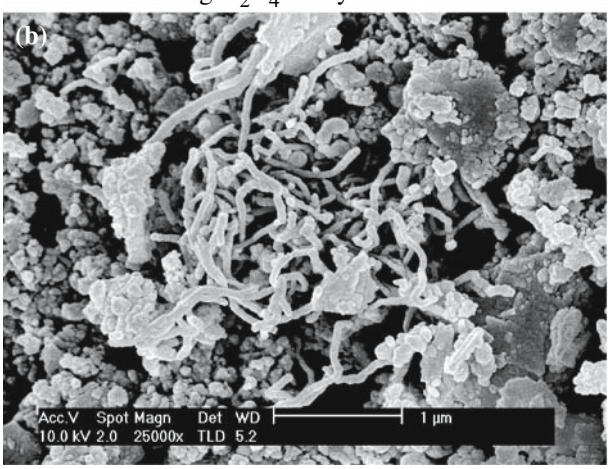

Figure 5. SEM images of used $Ni/Mgo–Al_2O_3$ and commercial $Ni/MgAl_2O_4$ catalyst.

4. Conclusions

$Ni/Mgo–Al_2O_3$ catalyst reveals high activity as well as stability in CSCRM, while the commercial Niα-alumina catalyst is not suitable for the reaction due to coke formation. The high activity and stability is mainly ascribed to the beneficial effects of MgO resulting from enhanced steam adsorption, basic property, fine dispersion of nano-sized NiO, and strong Ni to support interaction.

References

[1] J.R. Rostrup-Nielsen, in: *Catalysis, Science and Technology*, Vol. 5, eds. J.R. Anderson and M. Boudart (Springer, Berlin, 1984) pp. 1.
[2] H.-S. Roh, K.-W. Jun, W.-S. Dong, J.-S. Chang, S.-E. Park and Y.-I. Joe, J. Mol. Catal. A 181 (2002) 137.
[3] S.C. Tsang, J.B. Claridge and M.L.H. Green, Catal. Today 23 (1995) 3.
[4] A.T. Ashcroft, A.K. Cheetham, J.S. Foord, M.L.H. Green, C.P. Grey, A.J. Murrell and P.D.F. Vernon, Nature 344 (1990) 319.
[5] V.R. Choudhary, A.S. Mamman and D. Sansare, Angew. Chem. Int. Ed. Engl. 31 (1992) 1189.
[6] H.-S. Roh, W.-S. Dong, K.-W. Jun and S.-E. Park, Chem. Lett. (2001) 88.
[7] H.-S. Roh, K.-W. Jun, W.-S. Dong, S.-E. Park and Y.-I. Joe, Chem. Lett. (2001) 666.
[8] M.A. Peña, J.P. Gómez and J.L.G. Fierro, Appl. Catal. A 144 (1996) 7.
[9] Q.-H. Zhang, Y. Li and B.-Q. Xu, Catal. Today 98 (2004) 601.
[10] B.-Q. Xu, J.-M. Wei, H.-Y. Wang, K.-Q. Sun and Q.-M. Zhu, Catal. Today 68 (2001) 217.
[11] H.-S. Roh, H.S. Potdar and K.-W. Jun, Catal. Today 93–95 (2004) 39.
[12] H.-S. Roh, H.S. Potdar, K.-W. Jun, J.-W. Kim and Y.-S. Oh, Appl. Catal. A 276 (2004) 231.

[13] H.S. Potdar, H.-S. Roh, K.-W. Jun, M. Ji and Z.-W. Liu, Catal. Lett. 84 (2002) 95.
[14] A.A. Lemonidou, M.A. Goula and I.A. Vasalos, Catal. Today 46 (1998) 175.
[15] H.-S. Roh, K.-W. Jun, W.-S. Dong, S.-E. Park and Y.S. Baek, Catal. Lett. 74 (2001) 31.
[16] F. Cavani, F. Trifiro and A. Vaccari, Catal. Today 11 (1991) 173.
[17] L. Basini, A. Guarioni and A. Aragano, J. Catal. 190 (2000) 284.
[18] H.-S. Roh, K.-W. Jun, S.-C. Baek and S.-E. Park, Catal. Lett. 81 (2002) 147.
[19] H.-S. Roh, K.-W. Jun and S.-E. Park, Appl. Catal. A 251 (2003) 275.